Charge dispersion and recoil properties at $A = 131$ from the interaction of ^{197}Au with 11.5- and 300-GeV protons*

Y. W. Yu and N. T. Porile
Department of Chemistry, Purdue University, Lafayette, Indiana 47907
(Received 13 January 1975; revised manuscript received 24 February 1975)

Cross sections and thick-target recoil properties of five nuclides with $A = 131$ as well as those of a number of neighboring nuclides have been determined for the interaction of ^{197}Au with 11.5-GeV protons. The charge dispersion at $A = 131$ has a single peak at $Z_A - Z = -3.5$ and the total isobaric cross section is 8.9 ± 0.8 mb. The ranges indicate that only ~2% of this value can be ascribed to fission, the bulk of the cross section involving a deep spallation process. Similar data have been obtained at 300 GeV. Within the limits of error the results are the same at both energies. The systematics of deep spallation reactions are examined.

[NUCLEAR REACTIONS ^{197}Au(p,x), $A = 131$ products, $E = 11.5$ and 300 GeV; measured cross sections, recoil properties; deduced charge dispersion and properties of deep spallation.]

I. INTRODUCTION

The elucidation of the mechanisms responsible for the formation of products with $A \sim 100-150$ in the interaction of ^{238}U with multi-GeV energy protons has been a subject of recent interest. In contrast to intermediate energies ($E_p \sim 0.5$ GeV), where only binary fission contributes to the formation of products in this mass region, several mechanisms are of importance at GeV energies. In addition to fission, which leads primarily to the formation of neutron-excessive products, deep spallation which makes its main contribution to the formation of rather neutron deficient products is of importance. This process is thought to differ from ordinary spallation in that in additon to nucleons and light particles it involves the emission of more massive fragments, at least some of which appear to be preferentially emitted along the beam direction. In addition to these two mechanisms there may possibly be yet a third one, high deposition-energy fission, contributing to the formation of slightly neutron deficient nuclides. The information on these processes has been obtained, in the main, from charge dispersion[1-5] and recoil studies.[2,5-16] The combined use of both these techniques in a narrow mass range has been particularly informative.[2,5]

The characteristics of deep spallation have not been completely determined and because of the profusion of mechanisms active in interactions of multi-GeV protons with uranium this may not be the most suitable target for this purpose. A somewhat lighter target element having a much smaller fission cross section would thus be more suitable. We accordingly report here the results of a study of the charge dispersion and recoil properties of products in the $A \sim 130$ mass region formed in the interaction of ^{197}Au with 11.5-GeV protons. We have previously[5] performed a similar study for ^{238}U and a detailed comparison will be presented. Previous measurements on products in this mass region from the interaction of gold with multi-GeV energy protons are rather sparse. Rudstam and Sørensen[17] measured the yields of iodine nuclides, Hagebø and Ravn[18] those of antimony nuclides, Bächmann[19] those of various rare earth products, and Hudis *et al.*[20] those of xenon isotopes. Some of these data will be used in the interpretation of the present results.

We also report here the results of similar measurements performed with 300-GeV protons. The recent availability of protons in this new energy range has led to a number of comparative studies of cross sections and recoil properties determined at 300 and at 10–30 GeV[21-26] and the present data fall in this category.

II. EXPERIMENTAL

The procedure used in this work was essentially the same as that employed in our previous study of the formation of the products of interest from uranium. The complete procedure has been published[5] and only details of specific relevance to the present work are given below.

The 11.5-GeV proton irradiations were performed in the internal circulating beam of the zero gradient synchrotron (ZGS) at Argonne National Laboratory. The target stack consisted of 10-μm high-purity gold foil surrounded by three sets of 20-μm high-purity aluminum foil. The inner Al foils served as recoil catchers, the middle ones as beam intensity monitors, and the outer ones as

guards. The foils were carefully aligned to insure that they intercepted the same number of protons. We have previously established that under these conditions the loss of recoils from the target edge is negligibly small (<2%).

Two types of experiments were performed. The first was designed to yield data for ^{131}Ce, ^{131}La, and ^{131}Ba and involved 10-min irradiations followed by rapid radiochemical chain-breaking separations. Following separation ^{131}Ce and ^{131}La were allowed to decay to ^{131}Ba and the latter was assayed. The second type of experiment was intended to provide data for ^{131}I, ^{131}Cs, and ^{131}Ba (cumulative), as well as for other I, Cs, and Ba nuclides. These experiments involved 20-min irradiations followed by radiochemical separation and activity measurements. The various nuclides were assayed by means of γ-ray or x-ray spectrometry performed with calibrated Ge(Li) detectors. The decay properties of the observed nuclides are summarized in Table I.

The 300-GeV irradiations were performed in the Neutrino Hall at the Fermi National Accelerator Laboratory. Four irradiations, each approximately 10 h long, were performed. The bombardments were discontinuous and corrections were applied for these discontinuities as well as for variations in beam intensity. The target stacks were made of the same material as those used in the ZGS bombardments and they were processed and assayed in the same manner as the latter.

TABLE I. Decay properties of observed nuclides. Unless otherwise indicated the values are from C. M. Lederer, J. M. Hollander, and I. Perlman, *Table of Isotopes* (Wiley, New York, 1967), 6th ed.

Nuclide	Half-life	Observed γ ray (keV)	Abundance (per 100 decays)
^{131}Ce^{m}	5 min [a]	216(^{131}Ba)	19
^{131}Ce^{g}	10 min [a]	216(^{131}Ba)	19
^{131}La	61 min [b]	216(^{131}Ba)	19
^{128}Ba	2.42 day	443(^{128}Cs)	27
^{131}Ba	11.5 day [c]	216	19
^{129}Cs	32.06 h	372	31.7 [d]
^{131}Cs	9.70 day	K x ray	76.5 [e]
^{132}Cs	6.59 day	668	99
^{123}I	13.20 h [f]	159	83
^{124}I	4.18 day	603	61.4 [g]
^{126}I	13.02 day [h]	388	34
^{130}I	12.30 h	538	99
^{131}I	8.06 day [i]	364	82

[a] A. E. Norris, G. Friedlander, and E. M. Franz, Nucl. Phys. 86, 102 (1966); M. A. Deplanque, C. Gerschel and N. Perrin, *ibid.* A207, 565 (1973).
[b] A. Spalek, I. Rezanka, J. Frana, J. Jursik, and M. Vobecky, Nucl. Phys. 118, 161 (1968).
[c] J. Fechner, A. Hammesfahr, A. Kuge, S. K. Sen, H. Toschinski, J. Voss, P. Wergt, and B. Martin, Nucl. Phys. 130, 545 (1969).
[d] D. J. Horen, Nucl. Data B8, 123 (1972).
[e] Fluorescence yield = 0.88.
[f] R. L. Auble, Nucl. Data B7, 363 (1972).
[g] F. E. Bertrand, Nucl. Data B10, 91 (1973).
[h] R. L. Auble, Nucl. Data B9, 125 (1973).
[i] G. Graeffe and W. B. Walters, Phys. Rev. 153, 1321 (1967).

III. RESULTS

A. 11.5-GeV data

The results are summarized in Table II which lists the nuclides of interest, the nature of the observed yield, i.e., cumulative (C) or independent (I), the formation cross sections, and the recoil properties. The cross sections are based on a value of 8.6 mb for the ^{27}Al(p, $3pn$) monitor reaction cross section.[27] We have previously ascertained[5] that the effect of secondaries on the measured cross sections is negligibly small (<2%) for the relatively thin targets used in this experiment. The quoted uncertainties are based on the agreement between the indicated number of replicate determinations. Additional systematic uncertainties in the cross sections arising from those in detector efficiencies and branching ratios are expected to be small (~5%) for all but ^{131}Ce. An additional (10–20)% uncertainty is likely for the latter due to uncertainties[5] in the half-lives and decay modes of the two short-lived isomers of ^{131}Ce.

There are very few data available for direct comparison with the present results. Rudstam and Sørensen[17] measured the yields of several iodine nuclides from the interaction of gold with 18 GeV protons. Their cross sections for ^{123}I(C) and ^{124}I(I) are 6.9 ± 0.6 and 0.23 ± 0.03 mb, respectively, in very good agreement with the present results.

The total isobaric cross section at $A = 131$ may be obtained with greatest accuracy from the ^{131}Ba(C) and ^{131}Cs(I) cross sections. It is apparent from Table II that the cross sections for the formation of more neutron-rich isobars are negligibly small. The resulting isobaric cross section is 8.9 ± 0.8 mb, where the uncertainty includes systematic as well as random errors. This value is in reasonably good agreement with that of 8.2 ± 0.5 mb reported by Hudis *et al.*[20] on the basis of a mass-spectrometric determination of the cumulative yield of ^{131}Xe at 29 GeV.

The tabulated recoil properties are the experimental range $2W(F + B)$, and the forward-to-backward ratio F/B. These quantities have their customary meaning, i.e., F and B are the fraction of the total activity of a given nuclide found in the forward or backward foils, respectively, and W is

TABLE II. Formation cross sections and recoil properties of $A \sim 131$ products from 11.5-GeV proton bombardment of gold. In column 3 the numbers in parentheses are the number of replicate determinations.

Product	Type of yield	σ (mb)	$2W(F+B)$ (mg/cm^2)	F/B
^{131}Ce	C	4.9 ± 0.4(3)	2.31 ± 0.14	2.19 ± 0.22
^{131}La	I	3.5 ± 0.4(3)	1.85 ± 0.25	2.07 ± 0.34
^{131}Ba	I	0.43 ± 0.12(3)	3.58 ± 1.14	1.90 ± 0.30
^{131}Ba	C	8.8 ± 0.3(5)	1.67 ± 0.07	2.16 ± 0.08
^{131}Cs	I	0.081 ± 0.010(2)	2.86 ± 0.05	1.81 ± 0.20
^{131}I	C	0.0014 ± 0.0004(2)		
^{128}Ba	C	6.3 ± 0.3(5)	1.93 ± 0.19	2.07 ± 0.20
^{129}Cs	C	8.6 ± 0.9(2)	1.53 ± 0.16	1.76 ± 0.17
^{132}Cs	I	0.031 ± 0.010(2)	3.49 ± 0.61	1.80 ± 0.30
^{123}I	C	7.4 ± 0.7(2)	1.73 ± 0.18	1.95 ± 0.03
^{124}I	I	0.26 ± 0.05(5)	2.86 ± 0.52	1.70 ± 0.24
^{126}I	I	0.066 ± 0.002(5)	4.10 ± 0.49	1.37 ± 0.05
^{130}I	I	0.0026 ± 0.0006(2)		

the target thickness. The ranges have been corrected by 3% for the effect of scattering at the target-catcher interface.[28] The uncertainties in the tabulated values are based on the agreement between replicate measurements.

The dependence of the ranges and F/B values on the distance from stability of the products in question is shown in Fig. 1. This distance is conveniently expressed as the difference between the most stable charge at mass number A, Z_A, and the effective charge of the product Z_{eff}. The effective charge of independent products is just their actual nuclear charge, while that of cumulative products requires a weighting by the cross sections of all isobaric precursors. These cross sections were estimated from the charge dispersion derived in the next section. The Z_A values were obtained[4] from a parabolic fit to isobaric masses.

The recoil ranges fluctuate about a value of 1.8 mg/cm^2 for $(Z_A - Z_{\text{eff}}) < -2$ and then increase rapidly as the products become less neutron deficient. The curve for products in this same mass region from uranium[5, 14, 25] is included for comparison and shows the same type of behavior. The large increase in range observed for the ^{238}U target between $(Z_A - Z_{\text{eff}})$ of −2.5 and 0 has been attributed[5] to a transition between deep spallation and fission. Evidently the same transition occurs for gold at nearly the same distance from stability. Although the low cross sections of neutron excessive products from gold precluded a determination of their recoil properties, an estimate of the range expected for fission can be obtained from 450-MeV data[29] as fission is the accepted mechanism for the formation of products in this mass region. The use of 450-MeV fission ranges at 11.5 GeV is reasonable since fission product ranges have been found[11] to be nearly independent of energy. The extrapolation to a value of 4.7 mg/cm^2 obtained in this fashion is consistent with the curve through the present data.

The F/B values decrease with increasing $(Z_A - Z_{\text{eff}})$ although the large uncertainties in some of the values make it difficult to determine the rate of decrease. The F/B values for uranium[5, 14, 25] display a similar trend although the ratios are much closer to unity than those for gold. This difference can be understood more readily in terms of the energy and momentum transferred to the struck nucleus by the incident proton. These quantities are derived from the recoil properties in the next section.

B. 300-GeV data

The results of the 300-GeV experiments are summarized in Table III. The cross sections are based on a value of 8.6 mb for the monitor reaction cross section[30] and all the data were processed in analogous fashion to the 11.5-GeV results. The ratios of cross sections and recoil properties at 300 GeV to the corresponding quantities obtained at 11.5 GeV are included in this table. The quoted uncertainties in these ratios are based on the random errors of the results obtained at each energy. Systematic errors cancel out because all measurements were made on the same γ rays with the same equipment. The various ratios are in most cases equal to unity within the limits of error. The weighted average values of the ratios were calculated using the reciprocals of the variances as the weighting factors. The results are $\langle \sigma_{300}/\sigma_{11.5} \rangle = 0.96 \pm 0.05$, $\langle 2W(F+B)_{300}/2W(F+B)_{11.5} \rangle = 1.01 \pm 0.11$, and $\langle (F/B)_{300}/(F/B)_{11.5} \rangle = 0.93 \pm 0.10$. The cross sections and F/B values

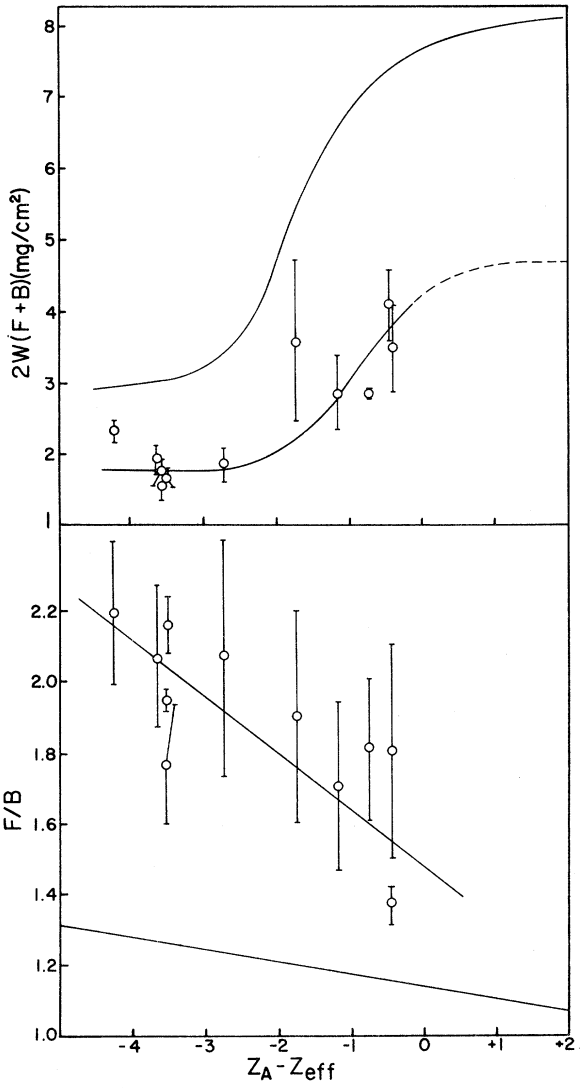

FIG. 1. Dependence of measured recoil properties on product ($Z_A - Z_{eff}$). The dashed extension of the curve drawn through the ranges is an estimate based on 450-MeV data. The curves without points are based on results for products in the same mass region from the interaction of ^{238}U with 11.5-GeV protons.

thus appear to be marginally smaller at 300 than at 11.5 GeV although the difference is within the experimental uncertainty.

The results may be compared with those previously reported[25] for products in the $A \sim 130$ mass region from uranium at 300 and 11.5 GeV. For this target the weighted average values for the nuclides listed in Table I are $\langle \sigma_{300}/\sigma_{11.5} \rangle = 0.83 \pm 0.12$, $\langle 2W(F+B)_{300}/2W(F+B)_{11.5} \rangle = 0.96 \pm 0.06$, and $\langle (F/B)_{300}/(F/B)_{11.5} \rangle = 0.99 \pm 0.05$. It thus appears that the cross section ratios for the products of interest are somewhat higher for gold than for uranium. In this respect the results for gold are closer to those obtained for vanadium,[21] cobalt,[21] and silver.[22,23] On the other hand, the recoil properties of these particular products are essentially independent of energy for both targets.

IV. DISCUSSION

A. Charge dispersion and recoil ranges at 11.5 GeV

The experimental cross sections may be used to construct a charge dispersion curve as shown in Fig. 2. The independent yields tabulated in Table II are plotted as a function of $Z_A - Z$. It is seen that for $Z_A - Z \gtrsim -2$ the yields drop off exponentially. The linear portion of the curve was drawn to pass through the ^{131}Ba, ^{131}Cs, and ^{131}I points. The ^{132}Cs and ^{130}I yields also fall on this line, while the ^{124}I and ^{126}I points lie somewhat above it. While the experimental yields narrowly define the charge dispersion for $(Z_A - Z) > -3$, the lack of independent yields at smaller $(Z_A - Z)$ introduces an uncertainty in this part of the curve. The cumulative yield of ^{131}Ce as well as those of the other neutron deficient products may be used to delineate this portion of the curve. The curve in Fig. 2 predicts cumulative cross sections of ^{131}Ce, ^{129}Cs, ^{128}Ba, and ^{123}I that are in reasonably good agreement with the experimental values as shown in the insert to the figure. In making this comparison the experimental cross sections of products with $A < 131$ were increased by 0.2% per mass number to reflect a

TABLE III. Cross sections and recoil properties of products from the interaction of ^{197}Au with 300-GeV protons and their ratios to 11.5-GeV values. In column 3 the numbers in parentheses are the number of replicate determinations.

Nuclide	Mode of formation	σ (mb)	$\frac{\sigma_{300}}{\sigma_{11.5}}$	$2W(F+B)$ (mg/cm²)	$\frac{2W(F+B)_{300}}{2W(F+B)_{11.5}}$	F/B	$\frac{F/B_{300}}{F/B_{11.5}}$
^{123}I	C	6.7 ± 0.4(2)	0.90 ± 0.10	1.86 ± 0.38	1.07 ± 0.24	1.75 ± 0.03	0.90 ± 0.02
^{124}I	I	0.26 ± 0.03(3)	1.00 ± 0.22	3.30 ± 0.21	1.15 ± 0.22	1.47 ± 0.35	0.86 ± 0.24
^{126}I	I	0.066 ± 0.012(3)	1.00 ± 0.18				
^{131}I	C	0.0019 ± 0.0008(2)	1.36 ± 0.69				
^{129}Cs	C	7.9 ± 0.2(2)	0.92 ± 0.10	2.05 ± 0.24	1.34 ± 0.21	2.25 ± 0.10	1.28 ± 0.14
^{132}Cs	I	0.05 ± 0.02(2)	1.61 ± 0.83				
^{128}Ba	C	6.2 ± 0.1(4)	0.98 ± 0.05	1.79 ± 0.12	0.93 ± 0.11	2.10 ± 0.24	1.01 ± 0.15
^{131}Ba	C	8.3 ± 0.7(4)	0.94 ± 0.08	1.63 ± 0.12	0.98 ± 0.08	1.87 ± 0.25	0.86 ± 0.10

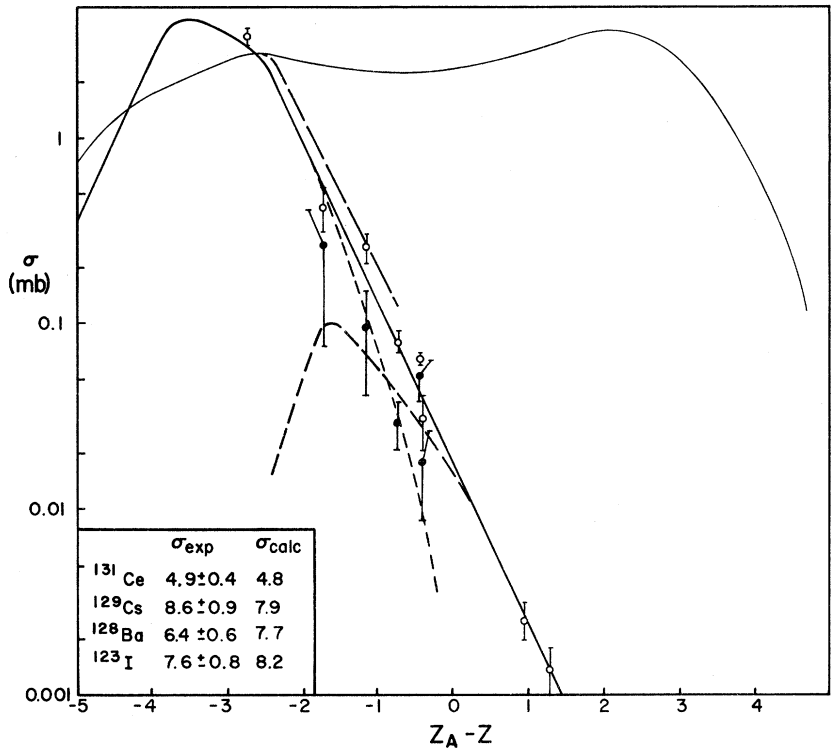

FIG. 2. Charge dispersion at $A = 131$ for the interaction of ^{197}Au with 11.5-GeV protons. The heavy solid curve is the charge dispersion as determined by the measured independent yields. The shape of the neutron deficient wing is determined by cumulative yields as shown in the tabular insert. The short dashed curves show the decomposition into deep spallation and fission. The light solid curve is the charge dispersion at $A = 131$ for ^{238}U and the long-dashed curve is the deep spallation portion of the latter. Open circles, measured independent yields; filled circles, deduced fission yields.

change of this magnitude in the total isobaric cross section as indicated by the results of Hudis *et al.*[20]

The charge dispersion at $A \sim 131$ peaks at $(Z_A - Z) \sim -3.5$ and has a full width at half-maximum of ~2 Z units. In view of the above uncertainty these values are not very well defined. The most interesting feature of the curve is the above noted exponential decrease in cross section for $(Z_A - Z) > -2$ which extends for over three orders of magnitude and corresponds to a factor of 7 decrease in yield per atomic number.

Bächmann[19] has measured the independent yields of ^{139}Ce and ^{139}Pr formed in the interaction of ^{197}Au with 28-GeV protons. These nuclides are sufficiently close in mass to those defining the present charge dispersion that their cross sections should be consistent with it. The reported independent yield of ^{139}Ce is 1.3 ± 0.6 mb, while that of ^{139}Pr is 1.5 ± 0.8 mb. The corresponding cross sections from Fig. 2 are 0.13 and 0.9 mb, respectively. The reported yield of ^{139}Ce thus is inconsistent with the present data. To be sure, the bombarding energies are not the same but the large body of high-energy data suggests that there should be little change in cross sections between 10 and 30 GeV. Hudis *et al.*[20] attempted to measure independent yields of ^{129}Xe and ^{131}Xe from the interaction of gold with 29-GeV protons but were only able to obtain upper limits of 0.3 and 0.1 mb, respectively. Our charge dispersion predicts values of 0.04 and 0.01 mb, respectively, which are not inconsistent with the xenon limits. We are aware of no other independent yields that could profitably be compared with the present results.

The charge dispersion at $A = 131$ was previously measured[5] for the interaction of 11.5-GeV protons with ^{238}U. The resulting curve is included in Fig. 2 for comparison. The two curves are vastly different for $(Z_A - Z) > -2$, the difference becoming as large as four orders of magnitude for positive $Z_A - Z$. This difference is, of course, a consequence of the much larger fission cross section of uranium. In our previous work[5] we decomposed the uranium charge dispersion curve into deep spallation and fission components on the basis of the measured ranges. The dashed curve in Fig. 2 indicates the deep spallation contribution and should thus be more comparable to the gold curve. The

two curves are indeed quite similar although the gold curve appears to peak at a somewhat higher Z and has a higher peak cross section. We defer further consideration of the relative cross sections to the next section, where the systematics of deep spallation are considered.

Although fission is of much less importance for gold than for uranium, it is not a completely negligible process. In fact, the binary fission cross section of heavy elements has been measured at multi-GeV energies,[31,32] and at 11 GeV the values for Au and U are 67 ± 10 and 1090 ± 140 mb, respectively.[32] It is of interest to determine the extent to which fission contributes to the $A = 131$ mass chain. The procedure developed for uranium,[2,5] in which the experimental recoil ranges are used to decompose the charge dispersion into deep spallation and fission components, may be employed. As indicated in the previous section, the spallation range is 1.8 mg/cm^2 and the fission range is 4.7 mg/cm^2. More precisely, the weighted mean range of the six very neutron deficient low-range products is 1.78 ± 0.23 mg/cm^2. It is assumed that products having intermediate ranges result from some particular combination of deep spallation and fission. The decomposition of the charge dispersion is shown in Fig. 2 as a plot of the fission cross sections of the five intermediate-range products. The uncertainties in these values are based on those in the measured cross sections and ranges as well as on those in the assumed deep spallation and fission ranges. The uncertainty in the fission range is estimated as ± 0.3 mg/cm^2. The dashed curves show the trend of the data but also reflect the additional constraint that the fission cross section must approach 0 as $Z_A - Z$ approaches -3 since this is the region where the low ranges characteristic of deep spallation are obtained. In spite of the large uncertainties associated with this decomposition it is clear that the fission curve is centered on the near neutron deficient side of stability and that this process becomes the dominant mechanism around stability. The integrated fission cross section is 0.2 ± 0.1 mb, which amounts to ~2% of the total isobaric yield at $A = 131$.

A similar decomposition[5] for $A = 131$ from ^{238}U yielded a fission cross section of 15.4 mb corresponding to 67% of the total isobaric yield. The ratio of the fission cross sections of ^{197}Au and ^{238}U at $A = 131$ thus is ~0.01 which is nearly an order-of-magnitude smaller than the corresponding ratio of the binary fission cross sections as determined by track measurements.[31,32] This difference is not surprising, since the fission yield curve for uranium peaks much closer to $A = 131$ than that for gold. The fact that the independent yields of ^{124}I and ^{126}I, which are in large measure formed by fission, lie above the $A = 131$ charge dispersion is consistent with this explanation.

B. Recoil parameters and systematics of deep spallation

The measured recoil properties may be used to derive values of various recoil parameters by means of the velocity vector model[6,28,29] embodying the two-step mechanism commonly invoked in high-energy reactions. According to this model the observed velocity of a recoil product $\vec{v}_I$ is resolved into components $\vec{v}$ and $\vec{V}$ corresponding to the cascade and deexcitation or breakup steps of the reaction, respectively. The component of $\vec{v}$ parallel to the beam direction is designated $v_\parallel$ and the ratio of its magnitude to that of the breakup velocity is denoted as $\eta_\parallel$. The breakup velocity must be symmetric in the moving system and is in fact assumed to be isotropic. Furthermore, if the range of a recoil in the target material R_I can be related to its velocity by an expression of the form

$$R_I = \text{const} \times v_I^N, \tag{1}$$

where N is a constant, the following relations can be derived:

$$2W(F+B) = R_0[1 + \tfrac{1}{4}\eta_\parallel{}^2(N+1)^2] \tag{2}$$

and

$$\frac{F}{B} = \frac{1 + \frac{2}{3}\eta_\parallel(N+2) + \frac{1}{4}\eta_\parallel{}^2(N+1)^2}{1 - \frac{2}{3}\eta_\parallel(N+2) + \frac{1}{4}\eta_\parallel{}^2(N+1)^2}. \tag{3}$$

The quantity R_0 is the mean range in the target material corresponding to the recoil speed V and the latter can be obtained from it by means of Eq. (1). In this fashion the mean kinetic energy $\langle T \rangle$, acquired by the observed products in the deexcitation step, can be obtained. These equations are based on a number of assumptions and approximations which are fully discussed elsewhere[33,34] and which can lead to (5–10)% uncertainties in the results.

The results of this analysis are summarized in Table IV. The range-velocity relation used to convert R_0 to $\langle T \rangle$ and to obtain the value of N was that developed by Cumming.[35] It is based on the tables of path lengths given by Northcliffe and Schilling[36] coupled with a semiempirical correction for the difference between path length and projected range. This relation yields $N = 1.98$ for the range values determined in the present work. The values of V and $\eta_\parallel$ may be used to obtain those of $v_\parallel$ and the latter may in turn be used to determine the average cascade deposition energies by the relation

$$E^* = 0.8 E_p A_{CN} v_\parallel / P_p \tag{4}$$

derived by Porile[37] from an analysis of 1.8-GeV

TABLE IV. Recoil parameters of $A \sim 131$ products from gold.

Nuclide	R_0 (mg/cm^2)	$\eta_{\parallel}$	$\langle T \rangle$ (MeV)	$v_{\parallel}$ [(MeV/amu)$^{1/2}$]	E^* (MeV)
^{131}Ce(C)	2.20± 0.17	0.147± 0.017	13.6± 1.6	0.0671± 0.0087	301± 38
^{131}La(I)	1.78± 0.25	0.137± 0.028	10.4± 2.7	0.0545± 0.0133	244± 59
^{131}Ba(I)	3.47± 1.14	0.121± 0.028	21.4± 13.2	0.0691± 0.0266	309± 118
^{131}Ba(C)	1.60± 0.07	0.145± 0.006	9.4± 0.8	0.0548± 0.0033	245± 14
^{131}Cs(I)	2.78± 0.05	0.112± 0.020	16.2± 0.6	0.0557± 0.0098	249± 44
^{128}Ba(C)	1.85± 0.19	0.137± 0.017	11.0± 2.1	0.0567± 0.0088	254± 40
^{129}Cs(C)	1.49± 0.16	0.106± 0.017	8.9± 1.8	0.0396± 0.0076	177± 34
^{132}Cs(I)	3.40± 0.61	0.111± 0.030	20.1± 6.8	0.0611± 0.0194	274± 86
^{123}I(C)	1.67± 0.18	0.126± 0.003	10.3± 2.1	0.0516± 0.0053	231± 24
^{124}I(I)	2.80± 0.52	0.100± 0.025	17.1± 6.0	0.0525± 0.0162	235± 72
^{126}I(I)	4.07± 0.49	0.059± 0.007	26.0± 6.0	0.0381± 0.0065	170± 29

Monte Carlo cascade calculations for heavy elements.[38] In this expression E_p and P_p are the kinetic energy and momentum of the incident proton and A_{CN} is the mass of the hypothetical compound nucleus. This relation has been shown to be invalid for deep spallation products from uranium[11,15] and its use in the analysis of the present data constitutes an attempt to delineate the limits of its validity.

Cumming and Bächmann[13] developed an analysis of deep spallation in which thick-target recoil ranges obtained for a variety of products from various targets may be systematized. The procedure, which is based on the application of random walk theory and momentum conservation to the deexcitation process, leads to an approximate value for the mean kinetic energy of the emitted particles $\langle t_t \rangle$ in terms of the target mass A_T, and the difference in mass between target and product ΔA. The relation is $\langle t_t \rangle = (A_T/\Delta A)\langle T \rangle$.

Figure 3 shows the variation of $\langle t_t \rangle$ and E^* with ΔA for a large number of deep spallation products. Included are the present results as well as the data of Yu and Porile[5,25] for products in the same mass region formed in the interaction of ^{238}U with 11.5-GeV protons, that of Panontin and Porile for nuclides in the $A = 100$–111 region from the interaction of ^{238}U[2] and ^{208}Pb[39] with 11.5-GeV protons, that of Cumming and Bächmann[13] for rare earth isotopes produced in the interaction of uranium and gold with 28-GeV protons, that of Starzyk and Sugarman[15] for similar products from ^{238}U plus 11.5-GeV protons, that of Neidhart and Bächmann[40] for rare earths from ^{181}Ta plus 19-GeV protons, and that of Chang, Cheney, and Sugarman[41] for tantalum nuclides formed in the interaction of 11.5-GeV protons with ^{209}Bi and ^{238}U. The inclusion of data at a variety of energies above 10 GeV is justified by the relative constancy of both recoil properties and cross sections at these energies. All these data were reanalyzed with the same range velocity and $E^* - v_{\parallel}$ relations as those used in the present work in order to make a meaningful comparison possible. In order to insure that only deep spallation products were included we restrict the analysis to products from U with $Z_A - Z_{\text{eff}} < -2.5$ and to products from the lighter targets with $Z_A - Z_{\text{eff}} < \sim -1$. As already noted, fission becomes important for products that are more neutron rich than that. We have also only included data for products having $\Delta A \gtrsim 30$, a mass loss that may safely be considered as a lower limit for deep spallation.

It is seen that the values of $\langle t_t \rangle$ increase in approximately linear fashion with ΔA, a trend that had already been observed by Cumming and Bächmann[13] on the basis of more limited data. This behavior can be qualitatively understood as a consequence of the relation between the nuclear temperature and the kinetic energy of evaporated particles. The mean kinetic energies are much larger than expected for processes involving only nucleon and light-particle emission indicating that massive fragments must be emitted with reasonably high probability. If this is indeed the case the values of $\langle t_t \rangle$ should actually be somewhat lower than indicated because the above formulation is based on the approximation that the mass of the first emitted particle may be neglected with respect to the target mass.

The values of E^* show a more complex dependence on ΔA although the scatter in the data is too large to permit any firm conclusions to be drawn. It does appear, however, that for reactions involving only moderate mass loss, $\Delta A < \sim 50$, the deposition energies increase with increasing mass loss. To a first approximation this is the behavior predicted by evaporation theory indicating that the $E^* - v_{\parallel}$ relation yields the correct dependence of E^* on ΔA. To be sure, the E^* values are much too low since they amount to only ~4 MeV/nucleon but at least the trend is correct. One could in fact easily increase the energy per emitted nucleon without unduly straining the $E^* - v_{\parallel}$ relation by in-

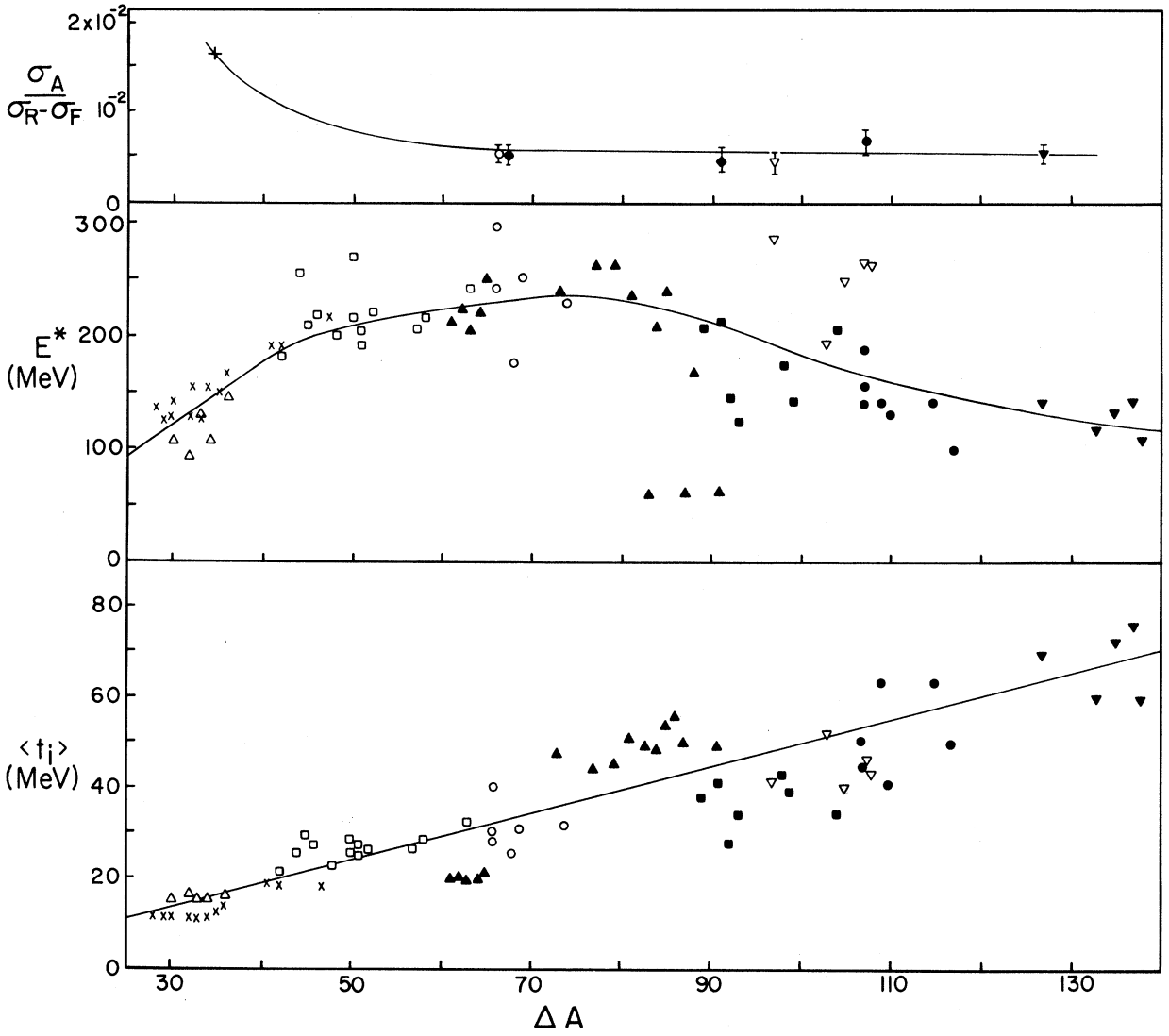

FIG. 3. Dependence of deep spallation properties on target-product mass difference ΔA. Top panel-fractional isobaric cross section; middle panel-average deposition energy; bottom panel-mean kinetic energy of emitted particles. The filled points refer to ^{238}U targets and come from the following sources: ▲, Refs. 15 and 41; ■, Ref. 13; ●, Refs. 5 and 25; ▼, Ref. 2; and ◆, Ref. 4. The open points are for ^{209}Bi, ^{208}Pb, or ^{197}Au targets and are taken from the following references: △, Ref. 41; □, Ref. 13; ○, present work; and ▽, Ref. 39. The crossed symbols refer to ^{181}Ta, the × referring to Ref. 40 and the + to Ref. 44.

creasing the numerical constant in this relation. Furthermore ΔA can be considerably overestimated by equating the residual nucleus from the cascade with the compound system and this leads to too low a value of $E^*/\Delta A$. The important point is that the two-step cascade-evaporation model as embodied in the $E^* - v_{\parallel}$ relation appears to work for reactions involving a mass loss of less than some 40 or 50 amu.

When ΔA increases beyond this point the situation becomes qualitatively different. The E^* values thus appear to level off and actually decrease for $\Delta A > \sim 80$. This behavior, which has been noted before, indicates that the $E^* - v_{\parallel}$ relation is not applicable to this situation. This may be the result of a change in the reaction mechanism, of a breakdown of the $E^* - v_{\parallel}$ relation at high deposition energies, or of a combination of both effects. If the formation of products with $\Delta A \gtrsim 50$ thus no longer involves ordinary spallation there is no *a priori* reason to expect E^* to continue to increase with ΔA. For instance, the deposition energies associated with the formation of fission products at 450 MeV[28] are independent of ΔA over a wide region.

The emission of light fragments, which is an im-

portant phenomenon at multi-GeV energies,[42] must be considered in this connection. It is generally believed that the heavy neutron deficient nuclides of present interest are, in fact, the residues of fragmentation. It is quite conceivable that the variation of E^* with ΔA is different for such a process than it is for spallation. Furthermore, since the light fragments appear to be preferentially emitted into the forward hemisphere in the frame of the moving struck nucleus[42,43] the residual nuclei may be left with anomalously low $v_{\parallel}$. The combination of these factors may thus account for the observed variation of E^* with ΔA.

We have so far focused on the energetics of deep spallation. It is also of interest to examine the dependence on ΔA of the total isobaric yield associated with this process. The data are rather sparse. In addition to the present result at $A = 131$ we can use the isobaric cross section reported for $A = 131$ from uranium,[5] those at $A = 111$ from ^{238}U[2] and ^{208}Pb,[39] those at $A = 147$ and $A = 171$ measured for the interaction of ^{238}U with 28-GeV protons[4] and similar results at $A = 146$ from tantalum.[44] The measured recoil ranges referred to above were used to insure that only deep spallation products were included in the isobaric cross sections.

When comparing different targets in this fashion one must take into account the differences in the total reaction cross section σ_R. Furthermore, the fission cross section σ_F changes by a large factor between tantalum and uranium and this difference must be taken into account in a determination of the probability of deep spallation. The most satisfactory measure of this probability appears to be the quantity $\sigma_A/(\sigma_R - \sigma_F)$ which gives the fraction of the nonfission decay channels leading to deep spallation products of mass A. In computing this quantity σ_R was evaluated by the usual geometric formula with $r_0 = 1.26$ fm, a value based on 24-GeV proton absorption measurements.[45] The values of σ_F are based on experimental measurements[31,32] and suitable interpolations. The results are summarized in the top panel of Fig. 3. The fractional deep spallation cross sections decrease between ΔA of 35 and 66 and remain essentially constant thereafter at a value of $5.5 \pm 0.8 \times 10^{-3}$. The decrease noted for moderate ΔA is typical of spallation and might be expected to continue if this were the main reaction mechanism for large ΔA. Although the paucity of the data does not permit an accurate determination of the ΔA value at which the fractional deep spallation yields level off it is nonetheless clear that this must occur in the same general region at which the E^* curve flattens out. It is thus tempting to ascribe both effects to the onset of deep spallation. If the region of constant fractional cross sections is assumed to extend over 100 amu then deep spallation must account for ~55% of the total nonfission cross section of heavy elements. For uranium this amounts to 620 mb, a value that is in close agreement with a previous[11] estimate of 600 mb for the fragmentation cross section. Once again, it is reasonable to identify deep spallation as the process forming the residual nuclei from fragmentation. It is of interest to note that while both the E^* and the cross section plots bear out a change in mechanism at $\Delta A \sim 50$, the $\langle t_t \rangle$ data do not. This may reflect fortuitous cancellations in the many averaging steps inherent in the derivation of this formalism.

V. CONCLUSIONS

We have measured the charge dispersion at $A = 131$ for the interaction of ^{197}Au with 11.5-GeV protons. The curve consists of a single peak at $(Z_A - Z) \sim -3.5$ and the total isobaric cross section is 8.9 ± 0.8 mb. With the aid of the measured recoil ranges we have decomposed the charge dispersion into deep spallation and fission components. Fission accounts for only $(2 \pm 1)\%$ of the total isobaric yield although it becomes the dominant mechanism at stability.

The systematics of deep spallation have been examined on the basis of the variation with target-product mass difference of the mean kinetic energy of the evaporated particles, the average deposition energy of the residual nuclei as calculated by the two-step reaction model, and the total isobaric cross section of low-range products. These correlations indicate that it is reasonable to identify these products as being the heavy residues from a fragmentation process. It appears that a mass loss of perhaps 50 amu is necessary before this process replaces conventional spallation as the dominant mechanism for the formation of neutron deficient products in the $A \sim 100$–170 mass region. The probability of deep spallation in nonfission high-energy reactions of heavy elements is $5.5 \pm 0.8 \times 10^{-3}$ per amu.

Cross sections and recoil properties of eight of the same nuclides determined at 11.5 GeV were also measured at 300 GeV. Within the limits of error the results are the same at both energies.

We wish to thank Dr. E. P. Steinberg for his continuing assistance with the ZGS irradiations, Dr. M. W. Weisfield for his help with the FNAL bombardments, and Dr. J. B. Cumming for a copy of his range-energy code.

*Work supported by the U. S. Atomic Energy Commission.

[1]G. Friedlander, L. Friedman, B. Gordon, and L. Yaffe, Phys. Rev. 129, 1809 (1963).
[2]J. A. Panontin and N. T. Porile, J. Inorg. Nucl. Chem. 32, 1775 (1970).
[3]E. Hagebø, J. Inorg. Nucl. Chem. 32, 2489 (1970).
[4]Y. Y. Chu, E. M. Franz, G. Friedlander, and P. J. Karol, Phys. Rev. C 4, 2202 (1971).
[5]Y. W. Yu and N. T. Porile, Phys. Rev. C 7, 1597 (1973).
[6]N. Sugarman, M. Campos, and K. Wielgoz, Phys. Rev. 101, 388 (1956).
[7]J. Alexander, C. Baltzinger, and M. F. Gadzik, Phys. Rev. 129, 1826 (1963).
[8]R. Brandt, in *Proceedings of the First International Symposium on the Physics and Chemistry of Fission, Salzburg 1965* (International Atomic Energy Agency, Vienna, Austria, 1965), Vol II, p. 329.
[9]V. P. Crespo, J. B. Cumming, and A. M. Poskanzer, Phys. Rev. 174, 1455 (1968).
[10]E. Hagebø and H. Ravn, J. Inorg. Nucl. Chem. 31, 2649 (1969).
[11]K. Beg and N. T. Porile, Phys. Rev. C 3, 1631 (1971).
[12]K. Bächmann and J. B. Cumming, Phys. Rev. C 5, 210 (1972).
[13]J. B. Cumming and K. Bächmann, Phys. Rev. C 6, 1362 (1972).
[14]Y. W. Yu, N. T. Porile, R. Warasila, and O. A. Schaeffer, Phys. Rev. C 8, 1091 (1973).
[15]P. M. Starzyk and N. Sugarman, Phys. Rev. C 8, 1448 (1973).
[16]Y. W. Yu and N. T. Porile (unpublished).
[17]G. Rudstam and G. Sørensen, J. Inorg. Nucl. Chem. 28, 771 (1966).
[18]E. Hagebø and H. Ravn, J. Inorg. Nucl. Chem. 31, 897 (1969).
[19]K. Bächmann, J. Inorg. Nucl. Chem. 32, 1 (1970).
[20]J. Hudis, T. Kirsten, R. W. Stoenner, and O. A. Schaeffer, Phys. Rev. C 1, 2019 (1970).
[21]S. Katcoff, S. B. Kaufman, E. P. Steinberg, M. W. Weisfield, and B. D. Wilkins, Phys. Rev. Lett. 30, 1221 (1973).
[22]G. English, Y. W. Yu, and N. T. Porile, Phys. Rev. Lett. 31, 244 (1973).
[23]G. English, Y. W. Yu, and N. T. Porile, Phys. Rev. C 10, 2281 (1974).
[24]S. K. Chang and N. Sugarman, Phys. Rev. C 9, 1138 (1974).
[25]Y. W. Yu and N. T. Porile, Phys. Rev. C 10, 167 (1974).
[26]S. B. Kaufman and M. W. Weisfield, Phys. Rev. C 11, 1258 (1975).
[27]J. B. Cumming, Annu. Rev. Nucl. Sci. 13, 261 (1963).
[28]N. Sugarman, H. Munzel, J. A. Panontin, K. Wielgoz, M. V. Ramaniah, G. Lange, and E. Lopez-Menchero, Phys. Rev. 143, 952 (1966).
[29]N. T. Porile and N. Sugarman, Phys. Rev. 107, 1410 (1957).
[30]M. W. Weisfield (private communication).
[31]J. Hudis and S. Katcoff, Phys. Rev. 180, 1122 (1969).
[32]R. Brandt, F. Carbonara, E. Cieslak, J. Piekarz, J. Zakrzewski, and H. Piekarz, Rev. Phys. Appl. 7, 243 (1972).
[33]J. M. Alexander, in *Nuclear Chemistry*, edited by L. Yaffe (Academic, New York, 1968), Vol. 1, p. 273.
[34]N. T. Porile, Phys. Rev. 185, 1371 (1969).
[35]J. B. Cumming (private communication).
[36]L. C. Northcliffe and R. F. Schilling, Nucl. Data A7, 233 (1970).
[37]N. T. Porile, Phys. Rev. 120, 572 (1960).
[38]N. Metropolis, R. Bivins, M. Storm, J. M. Miller, G. Friedlander, and A. Turkevich, Phys. Rev. 110, 204 (1957).
[39]J. A. Panontin and N. T. Porile, J. Inorg. Nucl. Chem. 33, 3211 (1971).
[40]B. Neidhart and K. Bächmann, J. Inorg. Nucl. Chem. 34, 423 (1972).
[41]S. K. Chang, M. C. Cheney, and N. Sugarman, Phys. Rev. C 10, 2467 (1974).
[42]A. M. Poskanzer, G. W. Butler, and E. K. Hyde, Phys. Rev. C 3, 882 (1971).
[43]J. B. Cumming, R. J. Cross, Jr., J. Hudis, and A. M. Poskanzer, Phys. Rev. 134, B167 (1964).
[44]Y. Y. Chu, E. M. Franz, and G. Friedlander, Phys. Rev. C 10, 156 (1974).
[45]A. Ashmore, G. Cocconi, A. N. Diddens, and A. M. Wetherell, Phys. Rev. Lett. 5, 576 (1960).